IEEE Access
Multidisciplinary | Rapid Review | Open Access Journal

Received March 22, 2020, accepted April 15, 2020, date of publication April 21, 2020, date of current version May 6, 2020.

Digital Object Identifier 10.1109/ACCESS.2020.2989326

Adaptive Second Order Recursive Terminal Sliding Mode Control for a Four-Wheel Independent Steer-by-Wire System

BIN DENG[1], KE SHAO[2], AND HAN ZHAO[1]
[1]School of Automotive and Transportation Engineering, Hefei University of Technology, Hefei 230009, China
[2]Center for Artificial Intelligence and Robotics, Tsinghua Shenzhen International Graduate School, Tsinghua University, Shenzhen 518055, China

Corresponding author: Ke Shao (shao.ke@sz.tsinghua.edu.cn)

This work was supported by the Fundamental Research Funds for the Central University of China under Grant PA2019GDZC0101.

ABSTRACT An adaptive second order recursive terminal sliding mode (SO-RTSM) is developed for the steering angle control of a four-wheel independent steer-by-wire (4WI-SbW) system. A recursive sliding mode structure is presented based on which the reaching phase is eliminated. Moreover, the finite time convergence of the tracking error is guaranteed compared to common integral sliding mode control (ISMC). Furthermore, to suppress chattering, instead of a first-order sliding mode used in a conventional ARTSM controller, a second order nonsingular terminal sliding mode is adopted such that reaching control input is obtained in an integral form. The advantage of the proposed controller is that the chattering can be effectively reduced without decreasing the control accuracy. Experiments are carried out on a real 4WI-SbW vehicle to demonstrate the fast convergence rate and small chattering of the proposed controller.

INDEX TERMS Four-wheel independent steer-by-wire (4WI-SbW), recursive terminal sliding mode (RTSM), second order, chattering, adaptive control.

I. INTRODUCTION

Recently, steer-by-wire (SbW) system has been investigated in many works because of its advantages of an active steering operation. For example, adaptive control is adopted in [1], [2] based on the parameter identification of the SbW system. In [3], adaptive disturbance rejection control (ADRC) is discussed for the control of an SbW system at different ground friction levels. However, although the steering shaft is cancelled compared a traditional steering system, the kinematic relationship between two steered wheels is still fixed by rack and pinion steering mechanism in an SbW system. To achieve a more flexible steering control, four-wheel independent steer-by-wire (4WI-SbW) system has drawn many attentions.

The 4WI-SbW technology can be potentially applied in wheeled vehicles to realize a more intelligent and complex motion. In 2015, NASA adopted a four-wheel independent steering system in a modular robotic vehicle (MRV) developed for a space application. In 2019, the company of AEV Robotics introduced a lightweight modular vehicle system (MVS), where an electric four-wheel independent steering system is installed. In 2020, Jaguar Land Rover(JLR) launched a four-wheel individually-steered self-driving car ''Project Vector'' for an urban traffic environment. Compared to conventional steering system or SbW system, the mechanical connection between tire and steering wheel or between two tires are both cancelled where each tire is directly-steered by an individual motor [4]. Instead of a ''hard'' mechanical connection, flexible communication bus (such as CAN, FlexRay, etc.) is used for a ''soft'' connection. Since each tire is connected to an independent steering mechanism, it gets rid of the shortcomings and limitations of the traditional rack and pinion steering system and potentially improves the driving flexibility and safety [5], [6]. Explicitly, the 4WI-SbW system can provide the vehicle a smaller turning radius and a more flexible driving mode. At the same time, there exists a huge research prospects for the active safety control of a 4WI-SbW system installed vehicle. However, the vehicle is affected by many uncertainties at a real driving condition, and each steering tire is subject to a complex external disturbance. In the process of steering motion, if there exists a large wheel steering angle control error or a serious lag, tire sideslip

The associate editor coordinating the review of this manuscript and approving it for publication was Mark Kok Yew Ng.

and drag may occur, that will further aggravate tire wear, and the vehicle will not be able to drive normally in serious cases [7], [8]. Because of the uncertainty of the system parameters and the nonlinear characteristics of the tire, the controller design for a 4WI-SbW system is often a difficult work [9], [10]. Therefore, to obtain a desired steering angle control performance, robust controller with higher response speed and control accuracy is required.

Due to the advantages of fast convergence rate and strong robustness against system uncertainties, sliding mode control (SMC) has been widely used in many motion control systems such as feed drive system [11], mechanical transmission [12], automotive safety [13], etc. However, during the reaching phase, the system is sensitive to system uncertainties and noises and the sliding mode invariance can not be guaranteed any more [14]. Integral sliding mode technique (ISMC) provides a method to eliminate the reaching phase and as a result the global convergence time is also reduced [15], [16]. However, the conventional ISMC can only achieve asymptotic convenience since a linear sliding function is often used [17], [18]. In [19], motivated by ISMC, a recursive sliding mode structure is proposed based on which the finite time convergence is achieved but the singular problem may occur. In [20], nonsingular adaptive recursive terminal sliding mode (ARTSM) is first developed. However, the control input still contains a switching operation that may cause system chattering. As the main drawback of SMC, severe chattering may damage the mechanical structure or even make the system unstable. There exist several ways in the literatures to alleviate this phenomenon, e.g., boundary layer technique [21], disturbance compensation [22], filter technique [23], etc. The widely used boundary layer technique can lead to the loss of the invariance that defacts the control accuracy [21]. Alternatively, based on high order sliding mode (HOSM), the control input is obtained in an integration of the discontinuous switching term. The advantage of HOSM control is that the chattering is effectively suppressed while the sliding mode invariance maintains [24].

In this paper, activated by HOSM, an adaptive second order recursive terminal sliding mode (SO-RTSM) control method is proposed for the 4WI-SbW system. First, a dynamic model of the 4WI-SbW system with parametric uncertainty is presented. Second, based on the concept of ISMC, the controller is constructed based on a recursive integral terminal sliding mode. Moreover, a second order terminal sliding mode is combined in the recursive sliding mode to obtain a continuous reaching control input. Finally, to verify the superior advantages of fast convergence rate and small chattering of the proposed controller, experiments are conducted on a real 4WI-SbW vehicle compared to a conventional ARTSM controller. The main contribution of this paper is listed in the following:

(a) A recursive sliding mode structure is developed such that the reaching phase is eliminated and moreover, the finite time convergence of the tracking error to zero is ensured compared to ISMC.

(b) A second order nonsingular terminal sliding mode is introduced in the RTSM, based on which the reaching control input is achieved in an integral form of the signum function instead of a conventional switching term as that in ARTSM, which can effectively suppress chattering.

This paper is organized as follows. Section II presents the structure and the dynamic model of the 4WI-SbW system. In Section III, the SO-RTSM controller is discussed in detail where the stability analysis and parameter selection guideline are also provided. To demonstrate the advantages of proposed controller, section IV presents the experiment results on a real 4WI-SbW vehicle. Finally, conclusions and future work are given in Section V.

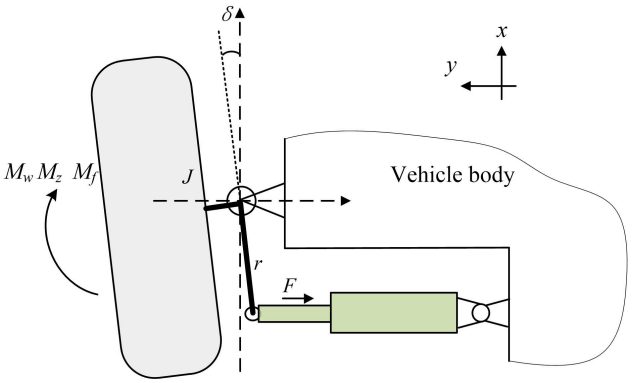

FIGURE 1. Force diagram of a single wheel (top view).

II. PLANT MODELING

In a four-wheel independent steer-by-wire (4WI-SbW) system, each tire is directly steered by a steering arm connected to an individual steering motor. As shown in Fig. 1, the plant model of each wheel can be described by

$$J\ddot{\delta} + c\dot{\delta} + k\delta = \tau + M_f + M_z + M_w \tag{1}$$

where δ is the steering angle of the wheel. J, c and k are the equivalent rotational inertia, damping and stiffness, respectively. M_w denotes the unknown uncertain ground torque. τ is the active steering torque impacted on the wheel given by

$$\tau = Fr\cos(\delta) \tag{2}$$

where F is the driving force of the steering motor and r is the radius of the steering arm. M_f is the friction torque given by

$$M_f = -T_v\dot{\delta} - T_c\, sgn(\dot{\delta}) \tag{3}$$

where T_v is the viscous friction coefficient, T_c is the viscous friction level and $sgn(\cdot)$ denotes the standard signum function. M_z is the tire alignment torque given by [25]

$$M_z = -F_z D\sin(2\gamma)\sin(\delta) \tag{4}$$

where F_z is the vertical tire force, D is the horizontal distance from the tire center to the kingpin and γ represents the kingpin inclination angle.

Substituting (2)–(4) to (1), the plant model can be reformed as

$$J\ddot{\delta} = Fr\cos(\delta) + M + M_w \tag{5}$$
$$M = -C\dot{\delta} - K\delta - T_c\, sgn(\dot{\delta}) - \xi \tag{6}$$

where $C = c+T_v, K = k+F_zD\sin(2\gamma), \xi = F_zD\sin(2\gamma)\Delta\delta$ and the relationship of $\sin(\delta) = \delta+\Delta\delta$ has been used with $\Delta\delta$ a small uncertain number.

In this paper, parameter uncertainties are assumed to satisfy

$$J = J_0 + \Delta J \tag{7}$$
$$C = C_0 + \Delta C \tag{8}$$
$$K = K_0 + \Delta K \tag{9}$$
$$T_c = T_{c0} + \Delta T_c \tag{10}$$

where $C_0 = c_0 + T_{v0}$, $K_0 = k_0 + F_{z0}D_0\sin(2\gamma_{r0})$. The symbol $\cdot_0$ represents the nominal value of each parameter and $\Delta\cdot$ denotes the corresponding uncertain value.

The control objective is to design a robust controller to achieve accurate and fast steering angle tracking performance of the 4WI-SbW system in the presence of system uncertainties. Define the tracking error

$$e = \delta - \delta_d \tag{11}$$

where δ_d is the steering angle command supposed to be thrice differentiable. Combining (11) with (5), the error dynamics is given by

$$J\ddot{e} = Fr\cos(\delta) + M + M_w - J\ddot{\delta}_d. \tag{12}$$

By substituting (8)–(10) into (12), the error dynamics can be rewritten as

$$J_0\ddot{e} = Fr\cos(\delta) + M_0 - J_0\ddot{\delta}_d + d. \tag{13}$$

where

$$M_0 = -C_0\dot{\delta} - K_0\delta - T_{c0}\, sgn(\dot{\delta}) \tag{14}$$
$$d = -\Delta J\ddot{e} - \Delta C\dot{\delta} - \Delta K\delta - \Delta T_c\, sgn(\dot{\delta}) - \xi - \Delta J\ddot{\delta}_d + M_w \tag{15}$$

with d the reformatted uncertainty to the system (13).

From (15), one can find that d is linearly affectly by δ and $\dot{\delta}$. Then, the derivative of d can reasonably be assumed to be bounded by

$$\frac{1}{J_0}\left|\dot{d}\right| < a_0 + a_1\left|\delta\right| + a_2\left|\dot{\delta}\right| + a_3\left|\ddot{\delta}\right| \tag{16}$$

where a_i $(i = 0, 1, 2, 3)$ is a positive number, which exists but are unknown.

III. CONTROL DESIGN

In this section, for the 4WI-SbW system to track the steering angle command fast and accurately under model uncertainties and disturbances, a robust controller based on an adaptive second order recursive terminal sliding mode (SO-RTSM) is presented. To achieve this goal, a recursive terminal sliding mode structure is constructed based on which the tracking error converges to the origin in finite while the reaching phase is eliminated. Moreover, an adaptive law is also introduced to compensate for the uncertainties without knowing the upper bound of the uncertainty a prior. Finally, selection of the control parameters is discussed.

A. CONSTRUCTION OF THE SO-RTSM CONTROLLER

To construct the controller, the following nonsingular terminal sliding function σ is first introduced as follows:

$$\sigma = \ddot{e} + \lambda_2\, sig(\dot{e})^{\gamma_2} + \lambda_1\, sig(e)^{\gamma_1} \tag{17}$$

where the parameters λ_1, λ_2 are selected such that the polynomial, which corresponds to the system (17), is Hurwitz. Besides, γ_1, γ_2 are selected to satisfy

$$\begin{cases} \gamma_1 \in (0, 1) \\ \gamma_2 = \dfrac{2\gamma_1}{1+\gamma_1} \end{cases} \tag{18}$$

The notation $sig(x)^a$ as first introduced in [26] is a simplified expression of

$$sig(x)^a = |x|^a\, sgn(x) \tag{19}$$

where $sgn(x)$ is the standard signum function. Note that for $a > 0$, $\forall x \in R$ the function $sig(x)^a$ is smooth and monotonically increasing and always returns a real number. It has been proven that when $\sigma = 0$ in (17), the tracking error e converges to zero in a finite time [27] (Referred to as t_σ).

Next, we propose a recursive integral terminal sliding function s as follows:

$$s = \sigma + \lambda\sigma_I \tag{20}$$

where σ is with (17), and σ_I is designed in the following form:

$$\dot{\sigma}_I = -\kappa\sigma_I + sgn(\sigma) \tag{21}$$

where the parameter $\kappa > 0$. In addition, to eliminate the reaching phase the initial integral value of σ_I in (20) is set as

$$\sigma_I(0) = -\lambda^{-1}\sigma(0). \tag{22}$$

By substituting (22) into (20), it can be verified that the initial sliding variable $s(0) = 0$ which implies that the control system is enforced to start on the sliding surface at the initial time such that the reaching time is eliminated [19]. Since the initial states of the 4WI-SbW system are available in practice, $\sigma_I(0)$ can be calculated by

$$\sigma_I(0) = -\lambda^{-1}\left(\ddot{e}(0) + \lambda_2\, sig(\dot{e}(0))^{\gamma_2} + \lambda_1\, sig(e(0))^{\gamma_1}\right). \tag{23}$$

When $s = 0$ holds in (20), the sliding variable σ converges to zero in a finite time t_s given by

$$t_s = \kappa^{-1}\ln\left(\frac{\kappa\,|\sigma(0)|}{\lambda} + 1\right) \tag{24}$$

The derivation of (24) is addressed in Appendix A.

Finally, we give the form of the SO-RTSM controller based on the recursive integral terminal sliding function. The controller will be constructed in the following form:

$$F = \frac{1}{r\cos(\delta)}(\tau_0 + \tau_1) \tag{25}$$

with τ_0, τ_1 the equivalent control input and the reaching control input to be designed, respectively.

By using (13), (17) and (20) and letting $\dot{s} = 0$, $d = 0$ in (13), we can obtain the following equivalent control input

$$\tau_0 = -M_0 + J_0\ddot{\delta}_d - J_0\left(\lambda_2\, sig(\dot{e})^{\gamma_2} + \lambda_1\, sig(e)^{\gamma_1} + \lambda\sigma_I\right). \tag{26}$$

Further, an integral form control input is introduced

$$\tau_1 = -J_0\int_0^t (\hat{a}_0 + \hat{a}_1\,|\delta| + \hat{a}_2\,|\dot{\delta}| + \hat{a}_3\,|\ddot{\delta}|)\, sgn(s) \tag{27}$$

where the control parameters $\hat{a}_0$, $\hat{a}_1$, $\hat{a}_2$ and $\hat{a}_3$ are updated by the following adaptive law

$$\dot{\hat{a}}_0 = \eta_0^{-1}\,|s| \tag{28}$$
$$\dot{\hat{a}}_1 = \eta_1^{-1}\,|\delta|\,|s| \tag{29}$$
$$\dot{\hat{a}}_2 = \eta_2^{-1}\,|\dot{\delta}|\,|s| \tag{30}$$
$$\dot{\hat{a}}_3 = \eta_3^{-1}\,|\ddot{\delta}|\,|s| \tag{31}$$

with $\eta_i > 0$ and $\hat{a}_i(0) \geq 0$, $(i = 0, 1, 2, 3)$.

Remark 1: An alternative dynamics of σ_I is utilized in (21) in addition to the power function form used in [20]. Although a signum function is adopted in (21), the control input (26) is continuous. Explicitly, the integral term σ_I is obtained due to the use of the second order sliding function (17).

Remark 2: In [20], a first-order nonsingular terminal sliding mode is utilized. However, serious chattering may occur due to the signum function in the reaching control input. In this paper, a second order sliding function is used such that an integral term is obtained in the reaching control input (27) instead of a conventional switching operation. Then, the total control input (25) is theoretically chattering-free, which will benefit control of the 4WI-SbW system.

B. STABILITY ANALYSIS

The result for the proposed SO-RTSM controller is summarized in the following theorem and stability analysis is provided.

Lemma 1: Given the 4WI-SbW system in (5) and the control law (25), there exists a positive number a_i in (16) such that $\hat{a}_i \leq a_i$ $(i = 0, 1, 2, 3)$ always holds.

Proof of Lemma 1 is in Appendix B.

Theorem 1: Consider the 4WI-SbW system in (5) with the parameter uncertainties (7)–(10). Then, under the SO-RTSM controller in (25), the tracking error e converges to zero in a finite time.

Proof: First, from (17), (20) and (25), the derivative of the sliding function s in (20) becomes

$$\begin{aligned}\dot{s} &= \dot{\sigma} + \lambda\dot{\sigma}_I \\ &= \dddot{e} + \lambda_2\gamma_2\,|\dot{e}|^{\gamma_2-1}\,\ddot{e} + \lambda_1\gamma_1\,|e|^{\gamma_1-1}\,\dot{e} + \lambda\dot{\sigma}_I \\ &= \frac{1}{J_0}\frac{d}{dt}\left(Fr\cos(\delta) + M_0 - J_0\ddot{\delta}_d + d\right) \\ &\quad +\lambda_2\gamma_2\,|\dot{e}|^{\gamma_2-1}\,\ddot{e} + \lambda_1\gamma_1\,|e|^{\gamma_1-1}\,\dot{e} + \lambda\dot{\sigma}_I \\ &= \frac{1}{J_0}\frac{d}{dt}\left(\tau_1 + d\right) \\ &= \frac{1}{J_0}(\dot{\tau}_1 + \dot{d})\end{aligned} \tag{32}$$

Next, choose the Lyapunov function as

$$V = \frac{1}{2}s^2 + \frac{1}{2}\sum_{i=0}^{3}\mu_i\tilde{a}_i^2 \tag{33}$$

where $\mu_i > 0, \tilde{a}_i = \hat{a}_i - a_i\,(i = 0, 1, 2, 3)$. Solving the derivative of (33) along the system trajectories and substituting (32) and (27) to it yields

$$\begin{aligned}\dot{V} &= s\dot{s} + \sum_{i=0}^{3}\mu_i\tilde{a}_i\dot{\tilde{a}}_i \\ &= s\frac{1}{J_0}(\dot{\tau}_1 + \dot{d}) + \sum_{i=0}^{3}\mu_i\tilde{a}_i\dot{\hat{a}}_i \\ &= s\frac{1}{J_0}\left(-(\hat{a}_0 + \hat{a}_1\,|\delta| + \hat{a}_2\,|\dot{\delta}| + \hat{a}_3\,|\ddot{\delta}|)\, sgn(s) + \dot{d}\right) \\ &\quad +\sum_{i=0}^{3}\mu_i\tilde{a}_i\dot{\hat{a}}_i \\ &\leq -(\hat{a}_0 + \hat{a}_1\,|\delta| + \hat{a}_2\,|\dot{\delta}| + \hat{a}_3\,|\ddot{\delta}|)|s| + \frac{1}{J_0}\,|\dot{d}|\,|s| \\ &\quad +\sum_{i=0}^{3}\mu_i\tilde{a}_i\dot{\hat{a}}_i \\ &\quad -(a_0 + a_1\,|\delta| + a_2\,|\dot{\delta}| + a_3\,|\ddot{\delta}|)|s| \\ &\quad +(a_0 + a_1\,|\delta| + a_2\,|\dot{\delta}| + a_3\,|\ddot{\delta}|)|s| \\ &= -(a_0 + a_1\,|\delta| + a_2\,|\dot{\delta}| + a_3\,|\ddot{\delta}| - \frac{1}{J_0}\,|\dot{d}|)|s| \\ &\quad +\mu_0\eta_0^{-1}\tilde{a}_0\,|s| + \mu_1\eta_1^{-1}\tilde{a}_1\,|\delta|\,|s| \\ &\quad +\mu_2\eta_2^{-1}\tilde{a}_2\,|\dot{\delta}|\,|s| + \mu_3\eta_3^{-1}\tilde{a}_3\,|\ddot{\delta}|\,|s| \\ &\quad -(\tilde{a}_0 + \tilde{a}_1\,|\delta| + \tilde{a}_2\,|\dot{\delta}| + \tilde{a}_3\,|\ddot{\delta}|)|s| \\ &= -(a_0 + a_1\,|\delta| + a_2\,|\dot{\delta}| + a_3\,|\ddot{\delta}| - \frac{1}{J_0}\,|\dot{d}|)|s| \\ &\quad +(\mu_0\eta_0^{-1} - 1)\,|s|\,(\hat{a}_0 - a_0) \\ &\quad +(\mu_1\eta_1^{-1} - 1)\,|\delta|\,|s|\,(\hat{a}_1 - a_1) \\ &\quad +(\mu_2\eta_2^{-1} - 1)\,|\dot{\delta}|\,|s|\,(\hat{a}_2 - a_2) \\ &\quad +(\mu_3\eta_3^{-1} - 1)\,|\ddot{\delta}|\,|s|\,(\hat{a}_3 - a_3)\end{aligned} \tag{34}$$

Note that $\hat{a}_i \leq a_i$ $(i = 0, 1, 2, 3)$ from Lemma 1, (34) becomes

$$\begin{aligned}\dot{V} \leq\ & -(a_0 + a_1\,|\delta| + a_2\,|\dot{\delta}| + a_3\,|\ddot{\delta}| - \frac{1}{J_0}\,|\dot{d}|)|s| \\ & -(\mu_0\eta_0^{-1} - 1)\,|s|\,|\hat{a}_0 - a_0| \\ & -(\mu_1\eta_1^{-1} - 1)\,|\delta|\,|s|\,|\hat{a}_1 - a_1| \\ & -(\mu_2\eta_2^{-1} - 1)\,|\dot{\delta}|\,|s|\,|\hat{a}_2 - a_2| \\ & -(\mu_3\eta_3^{-1} - 1)\,|\ddot{\delta}|\,|s|\,|\hat{a}_3 - a_3|\end{aligned} \tag{35}$$

Define the following symbols

$$\sigma_s = a_0 + a_1 |\delta| + a_2 \left|\dot{\delta}\right| + a_3 \left|\ddot{\delta}\right| - \frac{1}{J_0} \left|\dot{d}\right|$$
$$\sigma_i = (\mu_i \eta_i^{-1} - 1) \left|\delta^{(i)}\right| |s|$$

where $i = 0, 1, 2, 3$. Then, if σ_s, $\sigma_i > 0$, (34) can be rewritten as

$$\begin{aligned}\dot{V} &\leq -\sigma_s |s| - \sum_{i=0}^{3} \sigma_i |\tilde{a}_i| \\ &= -\sigma_s \sqrt{2} \frac{|s|}{\sqrt{2}} - \sum_{i=0}^{3} \sigma_i \sqrt{\frac{2}{\mu_i}} \sqrt{\frac{\mu_i}{2}} |\tilde{a}_i| \\ &\leq -\Upsilon \left(\frac{|s|}{\sqrt{2}} + \sum_{i=0}^{3} \sqrt{\frac{\mu_i}{2}} |\tilde{a}_i| \right) \\ &\leq -\Gamma V^{\frac{1}{2}} \end{aligned} \tag{36}$$

where Γ is a positive constant satisfying $\Gamma \leq \Upsilon$,

$$\Upsilon = \min \left\{ \sigma_s \sqrt{2},\ \sigma_i \sqrt{\frac{2}{\mu_i}} \right\} \tag{37}$$

It is obvious that $\sigma_s > 0$, and for any η_i $(i = 0, 1, 2, 3)$, Γ, there exist positive constants μ_i, a_i such that $\sigma_i > 0$, $\Upsilon \geq \Gamma$. Therefore, the inequality (36) satisfies the finite time stability criterion in Appendix C. More specific, V will converge from any initial condition $V(0)$ to zero in a finite time t_V given by

$$t_V \leq \frac{2V^{\frac{1}{2}}(0)}{\Gamma}. \tag{38}$$

This implies that the sliding variable s and the estimation error $\tilde{a}_i$ will converge to zero in a finite time as well. Besides, when $s = 0$, σ and e will successively converge to zero in the finite time of t_s and t_σ. Therefore, the tracking error e will converge from any initial condition to zero in the finite time of $t_c = t_V + t_s + t_\sigma$.

This completes the proof.

Remark 3: Based on the RTSM in (17) and (20), the system state passes along the sliding surfaces $s = 0$ and $\sigma = 0$ successively and as a result the tracking error converges to zero. As given in (22), $s(0) = 0$ can be assured by selecting an initial value of the integral element such that the reaching phase is eliminated. Moreover, different from the conventional ISMC [28], finite time convergence is achieved based on the proposed RTSM. Besides, when $s(0) = 0$, the value of $V(0)$ is also reduced and as a result the time for V to reach the origin, i.e., t_V is reduced from (38).

Remark 4: In practical applications, the sliding variable s is often chattering around zero and may result in conservatively large estimation of a_i as described in (28)–(31). To solve this problem, dead zone technique can be used for a practical implementation [29], [30]. The adaptive law is then given by

$$\begin{cases} \dot{\hat{a}}_i = \eta_i^{-1} \left|\delta^{(i)}\right| |s|, & \text{for } |s| > \epsilon \\ 0, & \text{for } |s| \leq \epsilon \end{cases} \tag{39}$$

where $i = 0, 1, 2, 3$, $\epsilon > 0$ is the threshold. It is clear from (39) that when s is within the threshold, $\hat{a}_i$ will retain its present value. One can verify that when $|s| < \epsilon$, (36) still holds, i.e., the finite-time stability is still guaranteed.

This completes the proof.

C. CONTROL PARAMETERS SELECTION

In a practical implementation, it has to compromise the impacts of control signal smoothness, energy consumption and measurement noises, etc. The control parameters selection guideline for the proposed SO-RTSM controller will be presented in the following and their values for the 4WI-SbW system will be selected.

1) Selections of λ_i, γ_i $(i = 1, 2)$: Large values of λ_i and γ_i in (17) lead to a faster convergence rate of e to zero along the sliding surface $\sigma = 0$. However, large values of them also cause an increased control input signal as given in (26). In this study, we choose $\lambda_1 = 100$, $\lambda_2 = 26$, $\gamma_1 = \frac{18}{35}$ and $\gamma_2 = \frac{36}{53}$.

2) Selections of λ, κ: As given in (24) and (26), a larger λ or κ in (20) indicates a smaller convergence time of σ after $s = 0$ but at the cost of an increased control input. Besides, a larger λ will also increase the amplitude of the integral element that implies a smaller steady-state tracking error. For the 4WI-SbW system, we choose $\lambda = 20$, $\kappa = 50$.

3) Selections of η_i $(i = 0, 1, 2, 3)$: The parameters η_i can be selected sufficiently small to achieve a fast estimation of the control gain as in (28)–(31). However, it may cause overestimation or even lead to control input saturation of the steering motor. Based on the experimental performance, we choose $\eta_0 = 0.5$, $\eta_1 = \eta_2 = \eta_3 = 2$.

IV. EXPERIMENTAL RESULTS

To demonstrate the proposed SO-RTSM controller for the 4WI-SbW system, experiments are carried out on a real 4WI-SbW vehicle shown in Fig. 2. The vehicle is with double-wishbone independent suspension and each wheel is

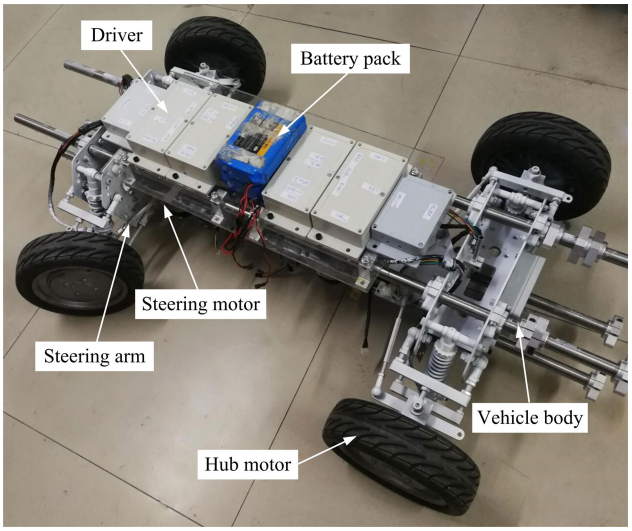

FIGURE 2. 4WI-SbW experimental vehicle.

driven by an independent hub motor. The steering angle of each wheel is obtained by the real-time working stroke of the steering motor. A magnetic navigation sensor is installed at the bottom of the experimental vehicle for detecting the lateral position error to a planed magnetic route. The proposed control algorithm is implemented in MATLAB/Simulink and runs on a dSPACE-DS1005 real-time platform with a sampling period of 5 ms. The software of ControlDesk installed on a PC is used to collect the experimental data from the dSPACE platform. Fig. 3 shows the control structure in the experiments.

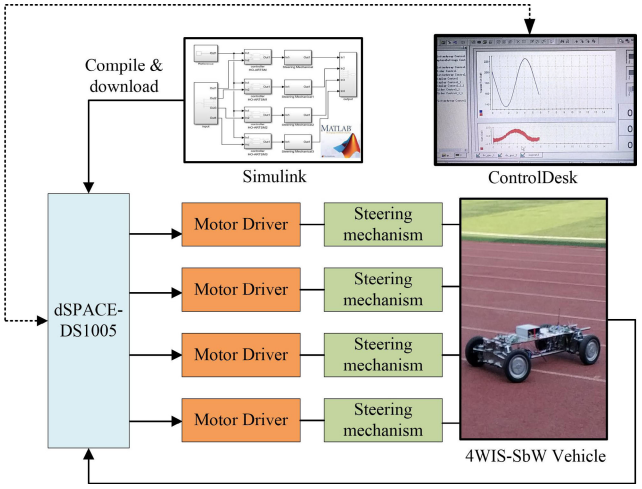

FIGURE 3. Control structure of the experiment.

A. STEERING CONTROL ROBUSTNESS TEST

To test the steering angle tracking performance under the proposed controller, the static experiment is studied for a single wheel on two different types of ground. The ARTSM controller is introduced for comparison, given by [20]

$$F_{ARTSM} = \frac{1}{r\cos(\delta)}(\tau_0 + \tau_1) \tag{40}$$

where

$$\tau_0 = -M_0 + J_0\ddot{\delta}_d - J_0(\varsigma\dot{e} + \gamma\alpha\,|e|^{\alpha-1}\,\dot{e} + \lambda\dot{\sigma}_I)$$
$$\tau_1 = -J_0(k_1 s + k_2\,sig(s)^{\mu} + (\hat{b}_0 + \hat{b}_1\,|\delta| + \hat{b}_2\,|\dot{\delta}|)\,sgn(s))$$

with the RTSM given by

$$s = \sigma + \lambda\sigma_I$$
$$\sigma = \dot{e} + \varsigma e + \gamma\,sig(e)^{\alpha}$$
$$\dot{\sigma}_I = sig(\sigma)^{\beta}$$

where the control parameters $\lambda, \varsigma, \gamma > 0$, $\alpha > 1$, $\beta > 0$, $k_1, k_2 > 0$, $\mu \in (0, 1)$; the initial integral value $\sigma_I(0) = -\lambda^{-1}\sigma(0)$; and $\hat{b}_0$, $\hat{b}_1$ and $\hat{b}_2$ are updated by

$$\dot{\hat{b}}_0 = \omega_0^{-1}\,|s|$$
$$\dot{\hat{b}}_1 = \omega_1^{-1}\,|\delta|\,|s|$$
$$\dot{\hat{b}}_2 = \omega_2^{-1}\,|\dot{\delta}|\,|s|$$

where $\omega_0, \omega_1, \omega_2 > 0$ and $\hat{b}_i(0) \geq 0$ $(i = 0, 1, 2)$.

The reference steering angle is a sinusoidal sweep signal with a time-varying amplitude and frequency.

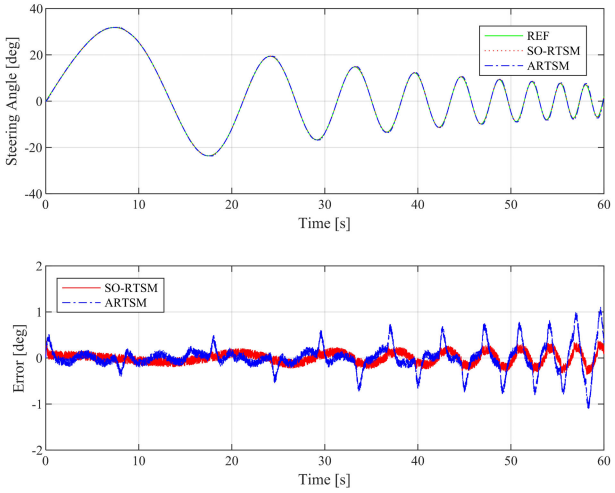

FIGURE 4. Steering angle profiles and tracking errors on an asphalt ground without load mass.

Case 1) Asphalt Ground Test:

A commonly used asphalt ground is first adopted. As we can see from Fig. 4, the tracking errors of both controllers increase as the frequency of the steering angle command grows and the peak error occurs when the steering direction changes. At either large amplitudes or high frequencies, the control accuracy of SO-RTSM is better than that of ARTSM. Specifically, the tracking error of ARTSM increases to 1.2 deg, which is much larger compared to that of SO-RTSM (0.4 deg). This is because the sliding error under the switching control input is increased due to the existence of the sampling period in a real discrete control system. As shown in Fig. 5, the control input of SO-RTSM responses faster than that of ARTSM. Moreover, due to the integral operation,

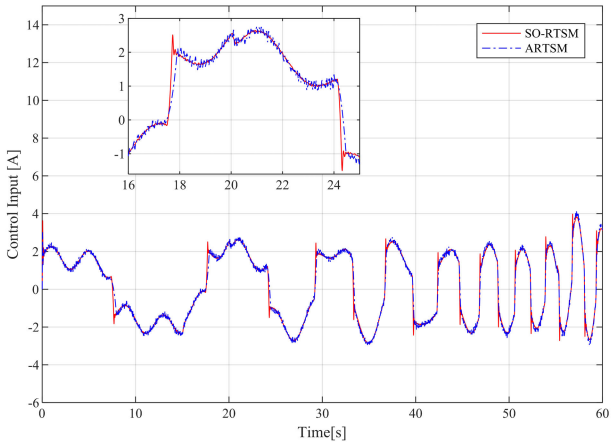

FIGURE 5. Control input variations on an asphalt ground without load mass.

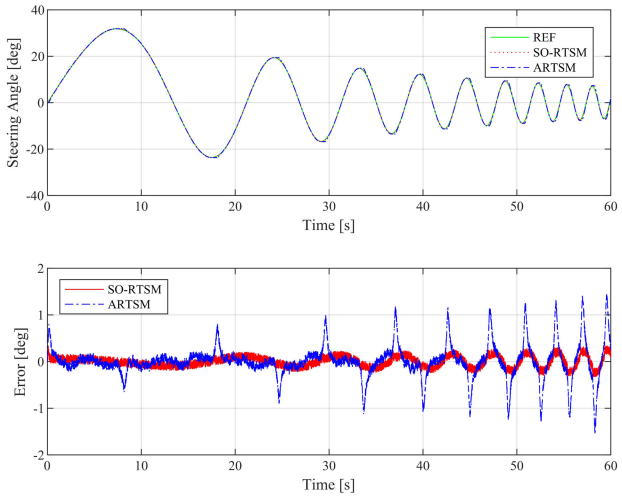

FIGURE 6. Steering angle profiles and tracking errors on a sandy ground with a load mass of 20 kg.

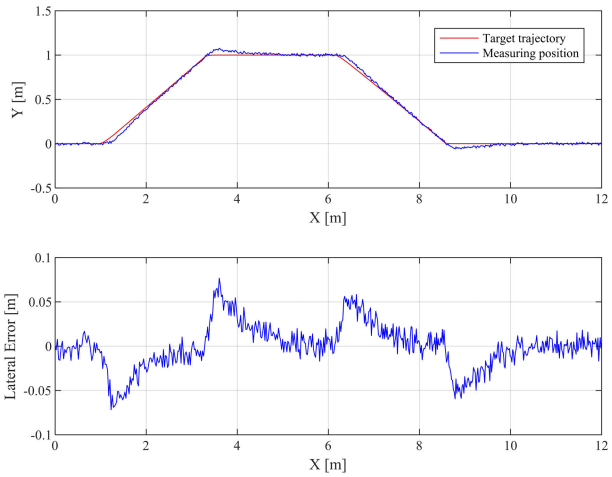

FIGURE 8. Position and lateral position error of the 4WI-SbW vehicle responses to the target path.

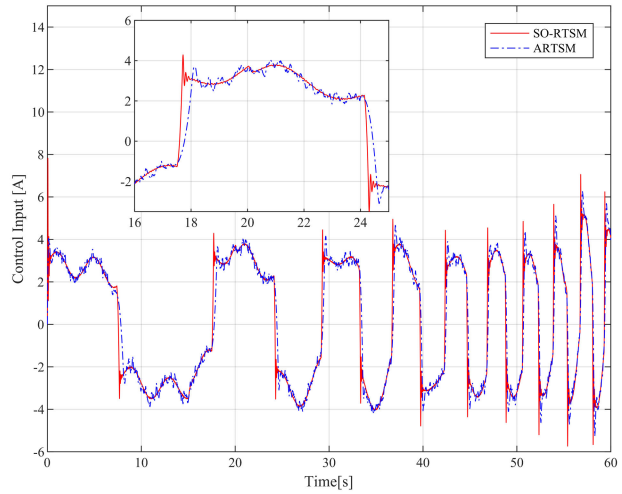

FIGURE 7. Control input variations on a sandy ground with a load mass of 20 kg.

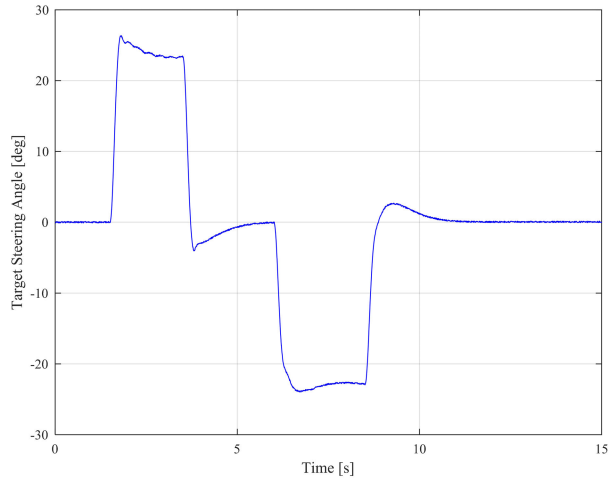

FIGURE 9. Target steering angle for each wheel to track.

the amplitude of the control input chattering of SO-RTSM is effectively suppressed compared to that of ARTSM.

Case 2) Sandy Ground Test:

To further test the robustness of the proposed controller, a sandy ground is adopted and a load mass of 20 kg is putted on the vehicle. It can be seen from Fig. 6 that the tracking error under ARTSM significantly increases compared to Case 1). To the contrary, under SO-RTSM controller, the tracking error is still limited under a small value of 0.4 deg. Similar to Case 1), the control input of SO-RTSM shows much smaller chattering than that of ARTSM as shown in Fig. 5. This experiment verifies the stronger robustness of the proposed controller compared to ARTSM.

B. PATH FOLLOWING PERFORMANCE

A crab-steering motion is used to test the steering angle tracking performance of four wheels under a dynamic uncertain environment. In a crab-steering motion, each wheel has the same steering angle such that the vehicle can complete a path following task without changing it heading angle. The crab-steering motion is potentially to realize a space-limited driving and the 4WI-SbW vehicle can reach the target position more quickly than that with a conventional steering system. The magnetic navigation control method is adopted in the experiment, where the a magnetic route has been placed on the ground for the vehicle to track. The lateral position error between the center of vehicle and the magnetic route is measured by the magnetic navigation sensor and a traditional PID control method is used to generate the target steering angle for each wheel to track.

As given in Fig. 8, the stable error of the vehicle lateral position under SO-RTSM controller is about ± 0.02 m and the maximum lateral error is less than 0.07 m. The reference steering angle signal from the PID controller is shown in Fig. 9 and the steering error of each wheel is

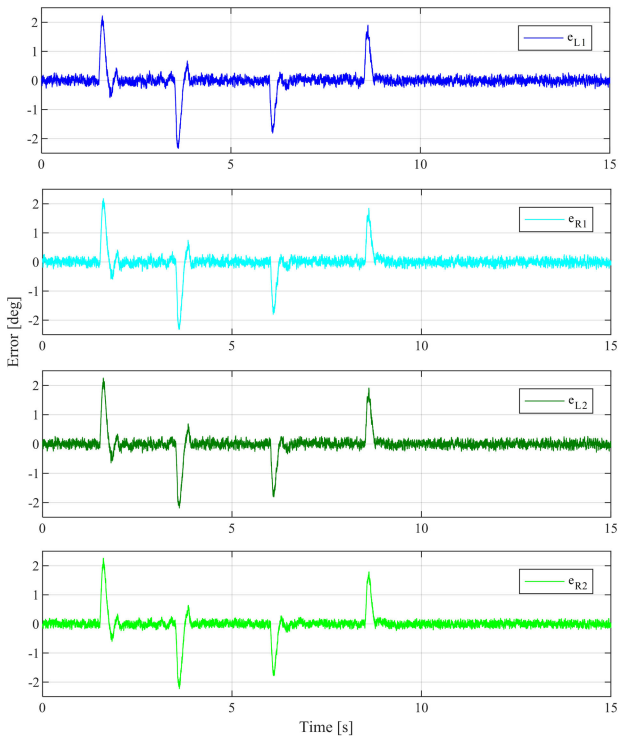

FIGURE 10. Steering angle tracking error of each wheel of the 4WI-SbW vehicle.

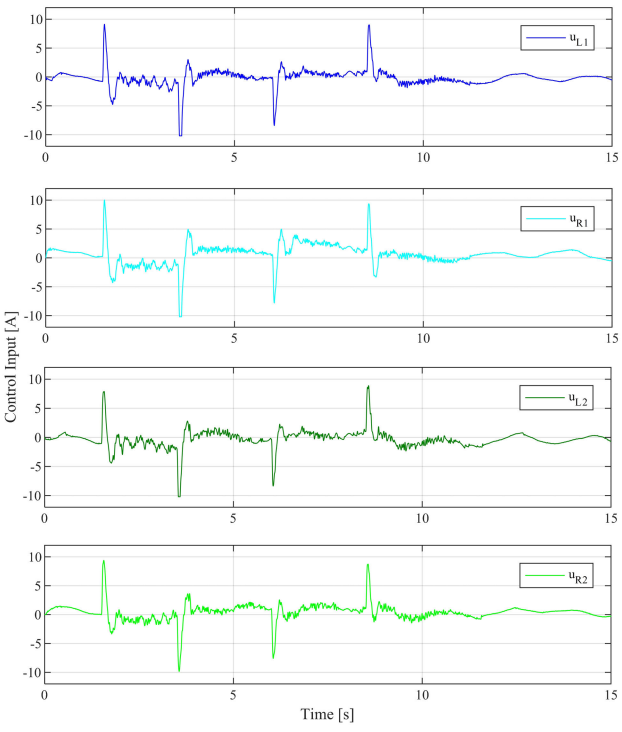

FIGURE 11. Control input variations of the 4WI-SbW vehicle.

given in Fig. 10. It can be seen that for each wheel, the peak error is under 2.2 deg and converges into a small stable error bound of around 0.25 deg within a short time of 0.3 s, which

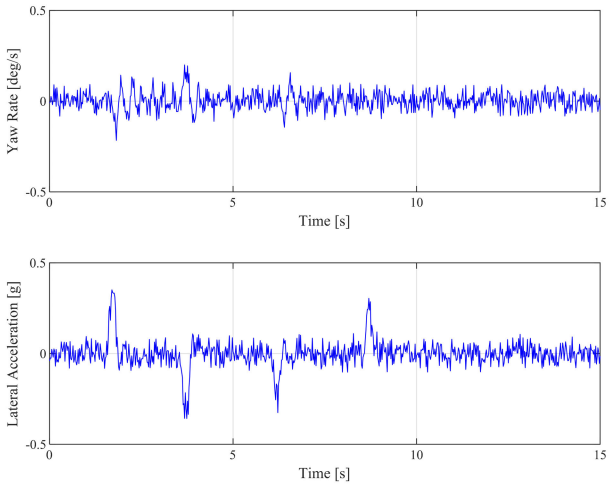

FIGURE 12. Yaw rate and lateral accelerations of the 4WI-SbW vehicle.

implies the good performance of the proposed controller for the 4WI-SbW control. The control input variations of four wheels are as shown in Fig. 11. One can find that the peak current is less than 10.05 A and occurs at the moment when the target steering angle changes its orientation (Fig. 9). Fig. 12 gives the yaw rate and lateral acceleration of the vehicle. More specific, the maximum yaw rate is below 0.18 deg/s and the stable yaw rate is around ± 0.1 deg/s that implies the vehicle heading angle changes small in the crab-steering motion. The dynamic crab-steering experiment demonstrate that the 4WI-SbW vehicle can accurately follow a desired path under the proposed SO-RTSM controller.

V. CONCLUSION

To improve the control performance of the 4WI-SbW system, an SO-RTSM controller is proposed in this paper. Lyapunov analysis proves that under the proposed controller, the steering angle error can converge to zero in finite time. Moreover, compared to conventional ARTSM, the proposed controller utilizes a second order nonsingular terminal sliding mode and as a result the reaching control input is obtained in a continuous form, which is useful to suppress the chattering of the control input signal. Besides, the proposed second order method maintains the sliding mode invariance during the sliding phase such that the control accuracy will not decrease when chattering is suppressed. In the future, we will do some work on the cooperative control strategy of four individual wheels and take the drive stability into account.

APPENDIX A

Once $s = 0$ holds in (20), it yields that $\sigma = -\lambda\sigma_I$, which implies that σ_I has the same convergence time as σ.

For (21), we have

$$\dot{\sigma}_I = -\kappa\sigma_I + sgn(\sigma). \tag{41}$$

1). For $\sigma < 0$, i.e., $\sigma_I > 0$, the equation (41) yields

$$1 = -\frac{\dot{\sigma}_I}{\kappa\sigma_I + 1}. \tag{42}$$

Let the time for σ_I to converge from $\sigma_I(0)$ to zero as t_s. By integrating bode sides of (42), we have

$$\begin{aligned} t_s &= -\int_{\sigma_I(0)}^{0} \frac{d\sigma_I}{\kappa\sigma_I + 1} \\ &= \kappa^{-1} \ln(\kappa\sigma_I(0) + 1) \\ &= \kappa^{-1} \ln(-\frac{\kappa\sigma(0)}{\lambda} + 1). \end{aligned} \tag{43}$$

2). For $\sigma > 0$, i.e., $\sigma_I < 0$, one can follow the above procedure and obtain

$$t_s = \kappa^{-1} \ln(\frac{\kappa\sigma(0)}{\lambda} + 1). \tag{44}$$

Therefore, it can be concluded that for any $\sigma(0) \neq 0$, σ converges to zero in the finite time given by

$$t_s = \kappa^{-1} \ln(\frac{\kappa\,|\sigma(0)|}{\lambda} + 1). \tag{45}$$

This completes the proof of (24).

APPENDIX B

Proof of Lemma 1: Supposing $|s| \neq 0$, from (28)–(31), $\hat{a}_i$ $(i = 0, 1, 2, 3)$ is increasing and there must exist a time instance t_1 such that

$$\hat{a}_0 + \hat{a}_1 |\delta| + \hat{a}_2 \left|\dot{\delta}\right| + \hat{a}_3 \left|\ddot{\delta}\right| > \frac{1}{J_0} \left|\dot{d}\right| \tag{46}$$

From (32), from $t = t_1$ the adaptation gain is sufficiently large to make the sliding variable s decreasing. Simultaneously, $\hat{a}_i(t)$ continues to increase until $s = 0$ is achieved in a finite time Δt. After that, $\hat{a}_i(t)$ will retain its final value $\hat{a}_i(t_1 + \Delta t)$. Due to its continuity property, $\hat{a}_i(t_1 + \Delta t)$ is finite, i.e., $\hat{a}_i(t)$ is upper bounded. Therefore, there exists a positive number a_i satisfying $\hat{a}_i \leq a_i$ in (16).

This completes the proof of Lemma 1.

APPENDIX C

Given the following first-order nonlinear differential inequality

$$\dot{V}(x) + \beta V^{\alpha}(x) \leq 0 \tag{47}$$

where $\beta > 0$, $0 < \alpha < 1$. $V(x)$ represents a positive Lyapunov function with respect to the state $x \in R$. Then, for any given initial condition $V(x(0)) = V(0)$, the function $V(x)$ converges to the origin in the finite time given by

$$t_V \leq \frac{V^{1-\alpha}(0)}{\beta(1-\alpha)}. \tag{48}$$

The derivation refers to [31], [32] and references therein.

REFERENCES

[1] A. Baviskar, J. R. Wagner, D. M. Dawson, D. Braganza, and P. Setlur, "An adjustable steer-by-wire haptic-interface tracking controller for ground vehicles," *IEEE Trans. Veh. Technol.*, vol. 58, no. 2, pp. 546–554, Feb. 2009.

[2] A. E. Cetin, M. A. Adli, D. E. Barkana, and H. Kucuk, "Implementation and development of an adaptive steering-control system," *IEEE Trans. Veh. Technol.*, vol. 59, no. 1, pp. 75–83, Jan. 2010.

[3] Z. Sun, J. Zheng, Z. Man, H. Wang, and R. Lu, "Sliding mode-based active disturbance rejection control for vehicle steer-by-wire systems," *IET Cyber-Phys. Syst., Theory Appl.*, vol. 3, no. 1, pp. 1–10, Mar. 2018.

[4] S. Yu, W. Li, W. Wang, and T. Qu, "Nonlinear control of active four wheel steer-by-wire vehicles," *IEEE Access*, vol. 7, pp. 127117–127127, 2019.

[5] P. Yih and J. C. Gerdes, "Modification of vehicle handling characteristics via steer-by-wire," *IEEE Trans. Control Syst. Technol.*, vol. 13, no. 6, pp. 965–976, Nov. 2005.

[6] M. Wan Choi, J. S. Park, B. Soo Lee, and M. Hyung Lee, "The performance of independent wheels steering vehicle(4WS) applied Ackerman geometry," in *Proc. Int. Conf. Control, Autom. Syst.*, Oct. 2008, pp. 197–202.

[7] F. Xu, X. Liu, W. Chen, and C. Zhou, "Dynamic switch control of steering modes for four wheel independent steering rescue vehicle," *IEEE Access*, vol. 7, pp. 135595–135605, 2019.

[8] T. Lun Lam, H. Qian, and Y. Xu, "Omnidirectional steering interface and control for a four-wheel independent steering vehicle," *IEEE/ASME Trans. Mechatronics*, vol. 15, no. 3, pp. 329–338, Jun. 2010.

[9] H. Wang, X. H. Gao, J. K. Chen, and C. Wang, "The impact of nonlinear of tire on multi-axle vehicle steering," *Adv. Mater. Res.*, vols. 403–408, pp. 3424–3429, Nov. 2011.

[10] H. Zhao, B. Wang, G. Zhang, and Y. Feng, "Energy saving design and control of steering wheel system of steering by wire vehicle," *IEEE Access*, vol. 7, pp. 44307–44316, 2019.

[11] X. Liu, H. Yu, J. Yu, and L. Zhao, "Combined speed and current terminal sliding mode control with nonlinear disturbance observer for PMSM drive," *IEEE Access*, vol. 6, pp. 29594–29601, 2018.

[12] H. Sheh Zad, T. I. Khan, and I. Lazoglu, "Design and adaptive sliding-mode control of hybrid magnetic bearings," *IEEE Trans. Ind. Electron.*, vol. 65, no. 3, pp. 2537–2547, Mar. 2018.

[13] H. Imine, L. M. Fridman, and T. Madani, "Steering control for rollover avoidance of heavy vehicles," *IEEE Trans. Veh. Technol.*, vol. 61, no. 8, pp. 3499–3509, Oct. 2012.

[14] K.-B. Park and T. Tsuji, "Terminal sliding mode control of second-order nonlinear uncertain systems," *Int. J. Robust Nonlinear Control*, vol. 9, no. 11, pp. 769–780, Sep. 1999.

[15] C. Yilmaz and Y. Hurmuzlu, "Eliminating the reaching phase from variable structure control," *J. Dyn. Syst., Meas., Control*, vol. 122, no. 4, pp. 753–757, Dec. 2000.

[16] V. D. Hajare, A. A. Khandekar, and B. M. Patre, "Discrete sliding mode controller with reaching phase elimination for TITO systems," *ISA Trans.*, vol. 66, pp. 32–45, Jan. 2017.

[17] Y. Pan, C. Yang, L. Pan, and H. Yu, "Integral sliding mode control: Performance, modification, and improvement," *IEEE Trans. Ind. Informat.*, vol. 14, no. 7, pp. 3087–3096, Jul. 2018.

[18] L. Zhou, Z. Che, and C. Yang, "Disturbance observer-based integral sliding mode control for singularly perturbed systems with mismatched disturbances," *IEEE Access*, vol. 6, pp. 9854–9861, 2018.

[19] C.-S. Chiu, "Derivative and integral terminal sliding mode control for a class of MIMO nonlinear systems," *Automatica*, vol. 48, no. 2, pp. 316–326, Feb. 2012.

[20] K. Shao, J. Zheng, K. Huang, H. Wang, Z. Man, and M. Fu, "Finite-time control of a linear motor positioner using adaptive recursive terminal sliding mode," *IEEE Trans. Ind. Electron.*, vol. 67, no. 8, pp. 6659–6668, Aug. 2020.

[21] Z. Sun, J. Zheng, Z. Man, and H. Wang, "Robust control of a vehicle steer-by-wire system using adaptive sliding mode," *IEEE Trans. Ind. Electron.*, vol. 63, no. 4, pp. 2251–2262, Apr. 2016.

[22] H. Rabiee, M. Ataei, and M. Ekramian, "Continuous nonsingular terminal sliding mode control based on adaptive sliding mode disturbance observer for uncertain nonlinear systems," *Automatica*, vol. 109, Nov. 2019, Art. no. 108515.

[23] H. Lee and V. I. Utkin, "Chattering suppression methods in sliding mode control systems," *Annu. Rev. Control*, vol. 31, no. 2, pp. 179–188, Jan. 2007.

[24] S. Mondal and C. Mahanta, "Adaptive second-order sliding mode controller for a twin rotor multi-input–multi-output system," *IET Control Theory Appl.*, vol. 6, no. 14, pp. 2157–2167, Sep. 2012.

[25] W. Yunchao, P. Feng, W. Pang, and M. Zhou, "Pivot steering resistance torque based on tire torsion deformation," *J. Terramechanics*, vol. 52, pp. 47–55, Apr. 2014.

[26] V. T. Haimo, "Finite time controllers," *SIAM J. Control Optim.*, vol. 24, no. 4, pp. 760–770, Jul. 1986.

[27] Y. Feng, F. Han, and X. Yu, "Chattering free full-order sliding-mode control," *Automatica*, vol. 50, no. 4, pp. 1310–1314, Apr. 2014.

[28] Y. Shtessel, C. Edwards, L. Fridman, and A. Levant, *Sliding Mode Control and Observation*. Cham, Switzerland: Springer, 2014.
[29] C. Edwards and S. Spurgeon, *Sliding Mode Control: Theory and Applications*. Boca Raton, FL, USA: CRC Press, 1998.
[30] V. I. Utkin, *Sliding Modes in Control and Optimization*. Cham, Switzerland: Springer, 2013.
[31] E. Moulay and W. Perruquetti, "Finite time stability and stabilization of a class of continuous systems," *J. Math. Anal. Appl.*, vol. 323, no. 2, pp. 1430–1443, Nov. 2006.
[32] F. Plestan, Y. Shtessel, V. Brégeault, and A. Poznyak, "New methodologies for adaptive sliding mode control," *Int. J. Control*, vol. 83, no. 9, pp. 1907–1919, Sep. 2010.

BIN DENG received the B.E. degree from the School of Automotive and Transportation Engineering, Hefei University of Technology, Hefei, China, in 2013, where he is currently pursuing the Ph.D. degree in automotive engineering.

His research interests include vehicle dynamics and control and sliding mode control.

KE SHAO received the B.E. and Ph.D. degrees from the School of Mechanical Engineering, Hefei University of Technology, Hefei, China, in 2013 and 2019, respectively.

From 2017 to 2019, he was a Visiting Scholar with the School of Software and Electrical Engineering, Swinburne University of Technology, Melbourne, VIC, Australia, founded by the China Scholarship Council. He is currently a Postdoctoral Research Fellow with the Tsinghua Shenzhen International Graduate School, Tsinghua University, Shenzhen, China. His research interests include mechanical system dynamics, sliding mode control, advanced robots, high-precision motion control, and vehicle dynamics and control.

HAN ZHAO received the Ph.D. degree from the Mechanical Engineering Department, Aalborg University, Denmark, in 1990.

He is currently a Professor and a Ph.D. Supervisor with the Hefei University of Technology, China. His research interests include mechanical transmission, magnetic machine, digital design and manufacturing, information systems, automobile design and manufacture, vehicle dynamics and control, and fuzzy control. He is a Committee Member of the International IFToMM Education Commission and an Editorial Member of the *Chinese Journal of Mechanical Engineering*.